F Hautmann

Perturbative RGE systematics in precision observables

- collaboration with V. Bertone and G. Bozzi

- based on

arXiv: 2407.20842 [hep-ph];

Phys. Rev. D 105 (2022) 096003 [arXiv:2202.03380].

Motivation:
the context of precision predictions at colliders

- Applications of QCD to collider physics involve solution of
  renormalization group equations (RGEs),
  e.g.: alpha-strong, PDFs, TMDs, . . .

- With the dramatic increase in accuracy of perturbative calculations
  for hard-scattering cross sections, theoretical systematic uncertainties
  from RGE solutions become potentially important.

- In many current applications these are not taken into account.

- We propose a method to deal with RGE systematics using the
  notion of "resummation scale" (borrowed from soft-gluon resummation
  literature).

Outline

1. Basic concepts of the methodology

2. Implications for precision observables:
   electroweak boson production
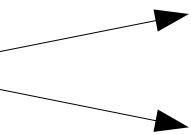   at the LHC and FCC-hh

Perturbative solution of RGEs: basic framework

$$\frac{d \ln R}{d \ln \mu}(\mu, \alpha_s(\mu)) = \gamma(\alpha_s(\mu))$$

where

$$\gamma(\alpha_s(\mu)) = \frac{\alpha_s(\mu)}{4\pi} \sum_{n=0}^{k} \left(\frac{\alpha_s(\mu)}{4\pi}\right)^n \gamma_n$$

For any truncation order k: difference between solutions which are formally equivalent at the nominal logarithmic accuracy but differ by subleading terms, and source RGE theory uncertainties.

- Practical applications:

  Analytic RGE solutions

  Numerical RGE solutions

- The goal is to devise strategies
  to evaluate truncation uncertainties in either case.

Physical picture (1)

RGE evolution →

M_ref   **M_phys**

Cf. variation of factorization and renormalization scales in perturbative QCD calculations:

$$\Sigma(Q) = f_i(\mu_F) \otimes h_{ij}(Q, \alpha_s(\mu_R), \mu_R/Q, \mu_F/Q) \otimes f_j(\mu_F)$$

- Varying muR and muF about Q takes into account missing higher orders to hard scattering function h

- RGE systematic uncertainties correspond to missing higher orders in RGE kernels for evolution from M_ref to M_phys in alpha-strong and f's.

Physical picture (2)

RGE evolution kernels, besides accomplishing the summation of large logarithms in the ratio of mass scales, in turn acquire dependence on kinematical variables, which may possibly be enhanced by QCD dynamics effects

- Example: x-dependence of QCD splitting functions (inverse Mellin transforms of the RGE kernels gamma for PDF evolution)

- 4-loop approximations to gluon splitting functions *[McGowan, Cridge, Harland-Lang, Thorne, Eur. Phys. J. C83 (2023) 185 [arXiv:2207.04739]]*

- $x \to 0, x \to 1$ asymptotics

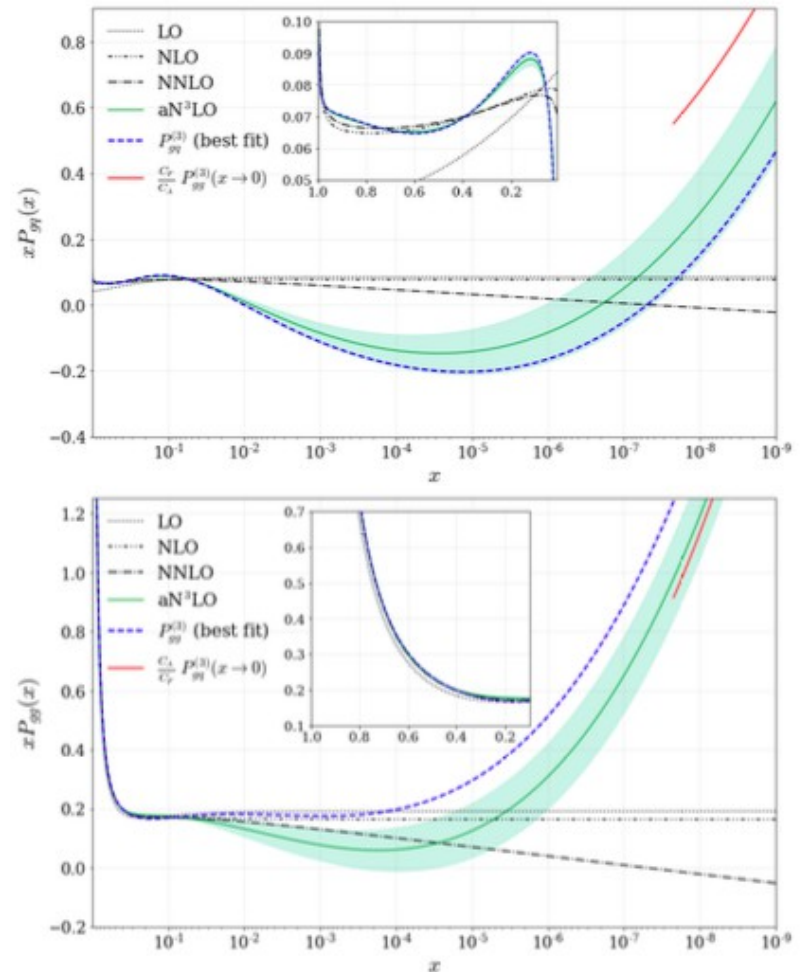- *[Moch et al; Falcioni et al; Gehrmann et al. 2022-2025]*

Figure 4: Perturbative expansions for the gluon splitting functions P_{gq} (top) and P_{gg} (bottom) including any corresponding allowed $\pm 1\sigma$ variation (shaded green region). The best fit value (blue dashed line) displays the prediction for this function determined from a global PDF fit.

Evaluating RGE systematics (1)

The "resummation scale" approach (analytic RGE solutions)

In the context of analytic solutions, this can be achieved using techniques borrowed from soft-gluon and transverse-momentum resummation [66–68]. Indeed, such solutions have the advantage of explicitly exposing terms proportional to $L_1 = a_s(\mu_0) \ln(\mu/\mu_0)$. Since μ_0 and μ are potentially far apart, L_1 can be large in spite of the presence of $a_s(\mu_0)$ and thus it cannot be treated as a perturbative parameter. This implies the need to sum powers of L_1 to all orders in perturbation theory. Once the analytic solution of the RGE has been obtained, one can decompose all instances of L_1 as follows,

$$L_1 = L_\kappa - a_s(\mu_0) \ln \kappa, \quad \text{with} \quad L_\kappa = a_s(\mu_0) \ln\left(\frac{\kappa\mu}{\mu_0}\right), \qquad (2.4)$$

where the scale $\kappa\mu$ is dubbed *resummation scale*. Provided that κ is of order $\mathcal{O}(1)$, the second term in the decomposition of L_1, *i.e.*, $a_s(\mu_0) \ln \kappa$, is perturbatively small. This allows one to expand the analytic solution of the RGE around $L_1 = L_\kappa$, retaining only terms within perturbative accuracy. The net result is an analytic solution that sums all powers of L_κ, while retaining powers of $a_s(\mu_0) \ln \kappa$ only up to the nominal accuracy. Variations of κ in the vicinity of $\kappa = 1$ generate subleading terms that provide an estimate of the perturbative uncertainty associated with the analytic solution of the RGE.

Evaluating RGE systematics (2)

The "shifted kernel" approach (numerical RGE solutions)

Make RG transformation:
$$\mu \to \xi\mu$$
$$\alpha_s(\mu) \to \alpha_s(\xi\mu)$$

consider the anomalous dimension γ truncated at NLO accuracy,

$$\gamma = a_s(\mu)\gamma_0 + a_s^2(\mu)\gamma_1 . \qquad (2.4)$$

Then we use the expanded solution for the running of the strong coupling to express $a_s(\mu)$ in terms of $a_s(\xi\mu)$, where ξ is a parameter of order $\mathcal{O}(1)$,

$$a_s(\mu) = a_s(\xi\mu) - a_s^2(\xi\mu)\beta_0 \ln \xi + \mathcal{O}(\alpha_s^3) , \qquad (2.6)$$

that plugged into Eq. (2.4) gives

$$\gamma = a_s(\xi\mu)\gamma_0 + a_s^2(\xi\mu) [\gamma_1 - \beta_0 \ln \xi] + \mathcal{O}(\alpha_s^3) , \qquad (2.7)$$

Variations of xi provide an estimate of the perturbative uncertainty associated with the numerical solution of the RGE.
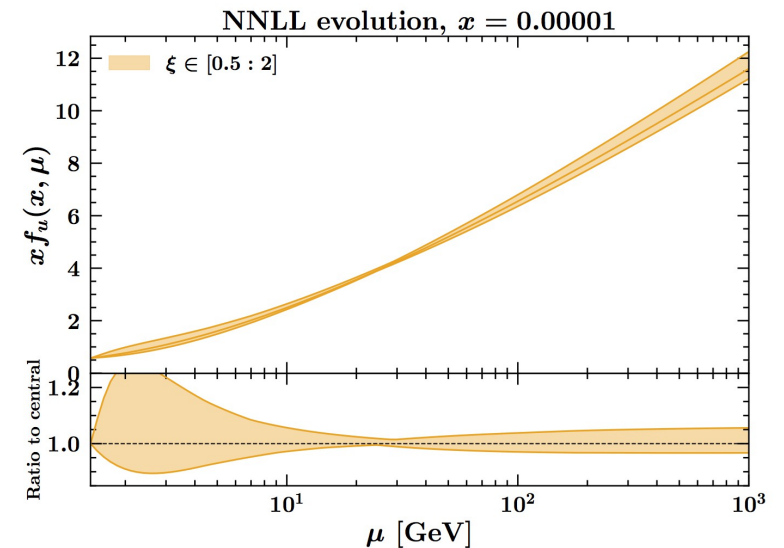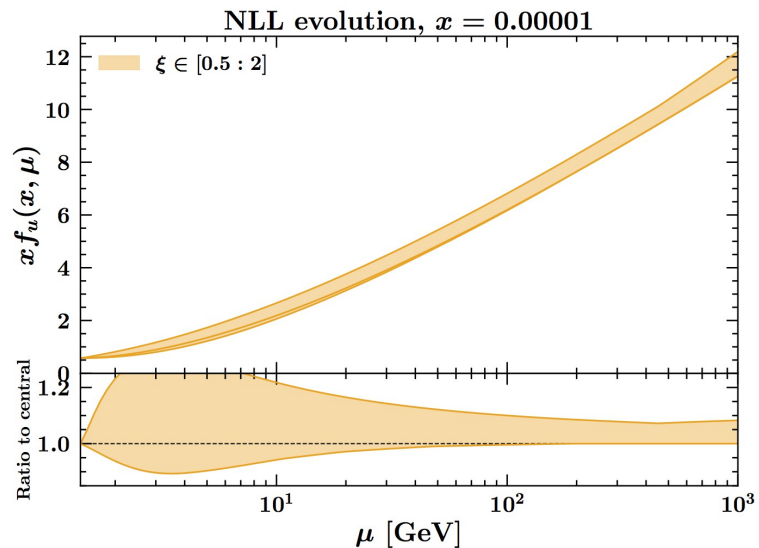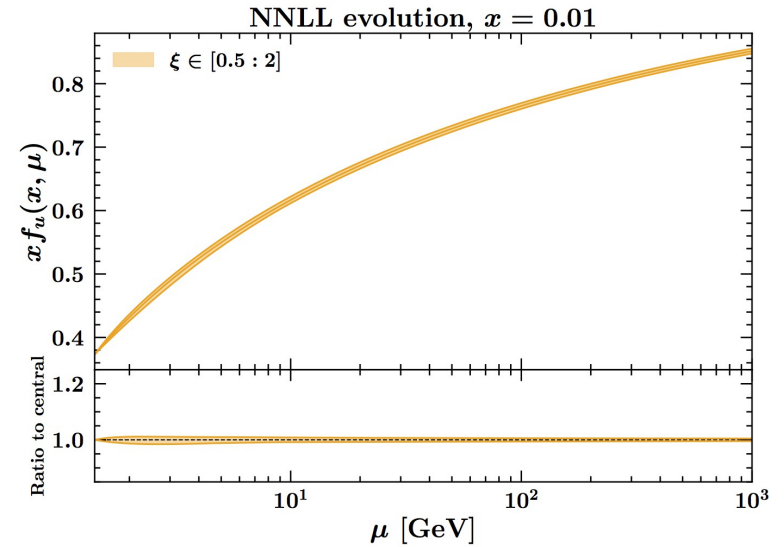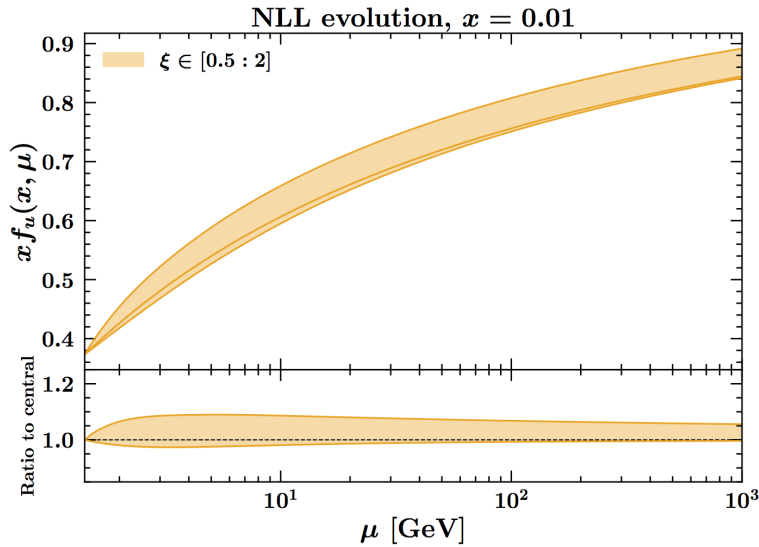
RGE systematics of the strong coupling
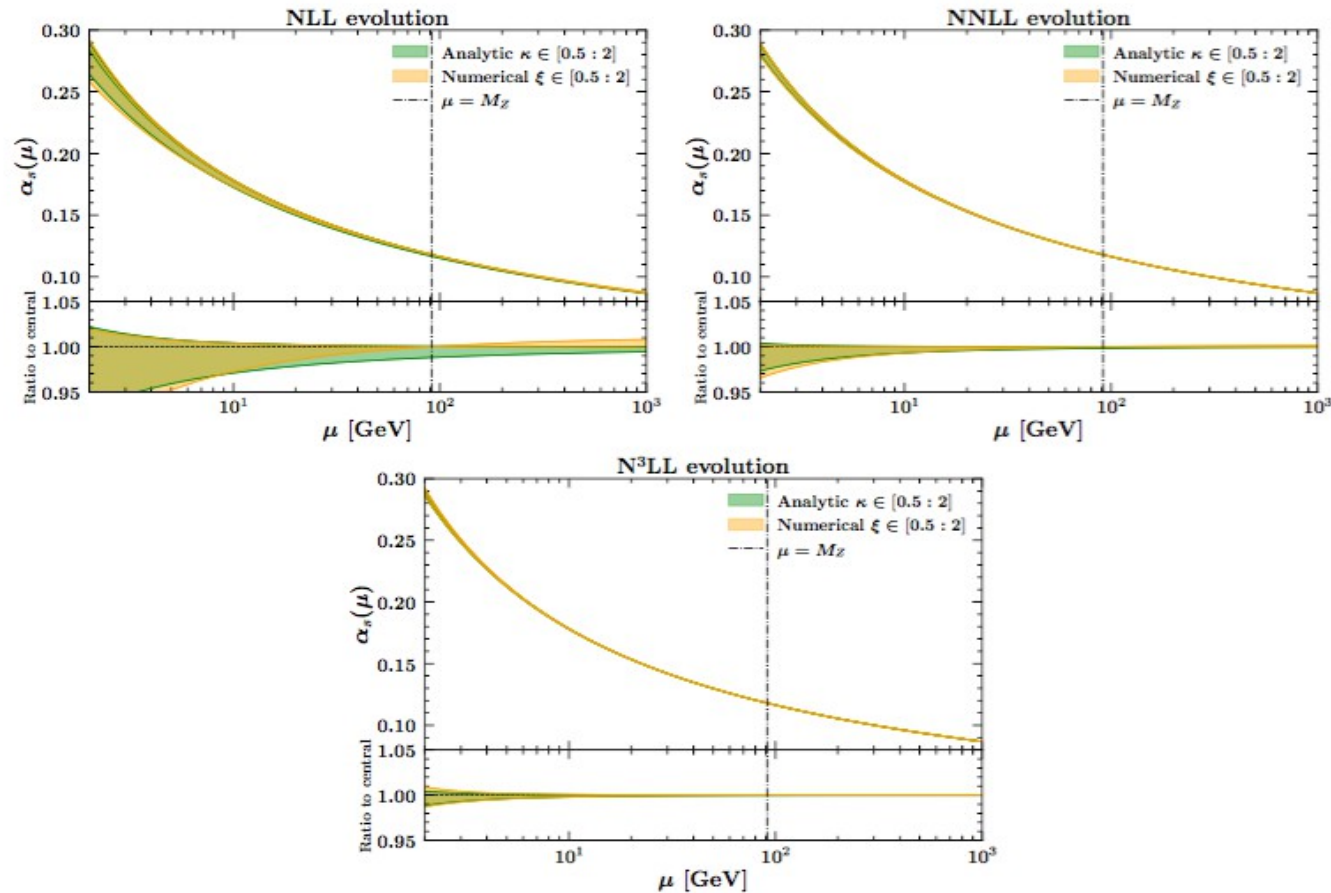
Figure 1. Analytic and numerical evolutions of the strong coupling α_s in the range $\mu \in [2 : 1000]$ GeV at NLL (top-left plot), NNLL (top-right plot), and N^{3}LL (bottom plot) accuracies. The boundary condition is set at $\alpha_s(M_Z) = 0.118$. Uncertainty bands correspond to variations of the parameters κ and ξ for analytic and numerical solutions, respectively, in the ranges $\kappa, \xi \in [0.5 : 2]$. Lower panels display the bands normalised to the respective central-value curves obtained with $\kappa = \xi = 1$. The vertical dot-dashed line indicates the scale $\mu = M_Z$ where the boundary condition is set. At this scale the uncertainty on numerical solutions reduces to zero.

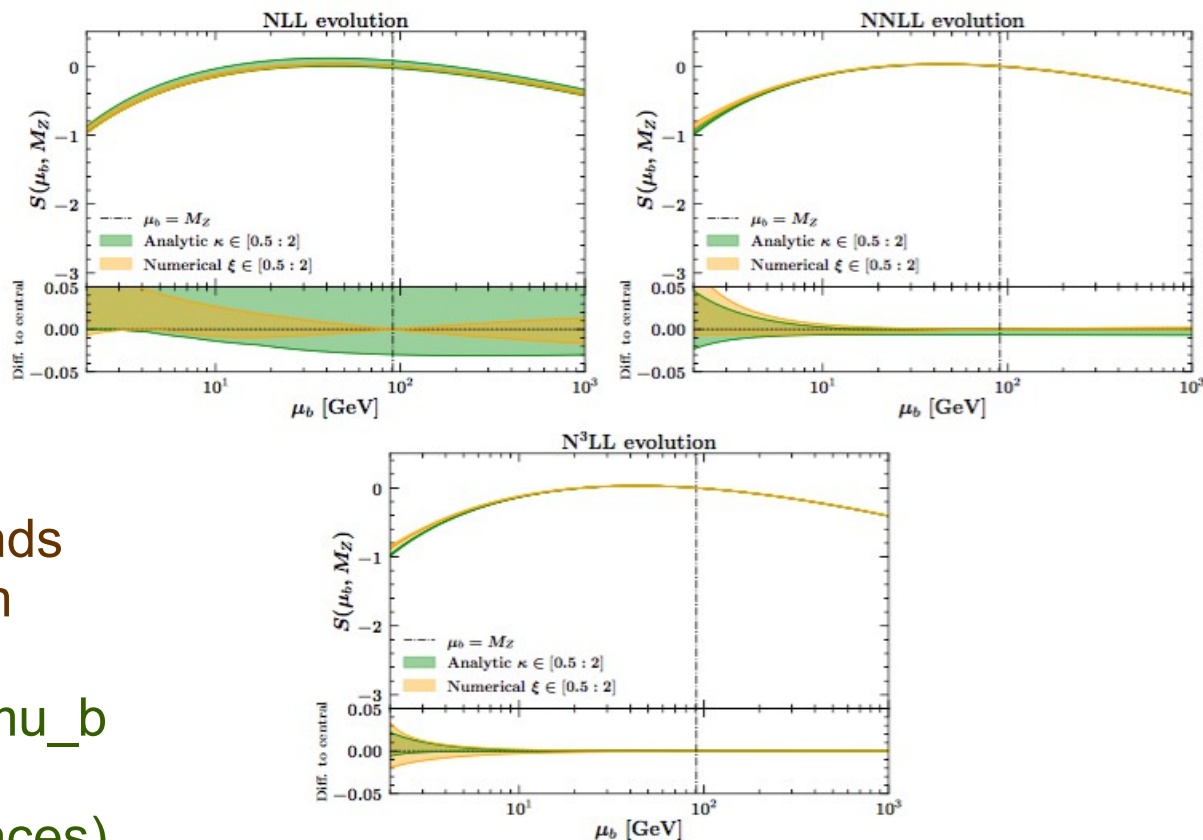# RGE systematics of the strong coupling
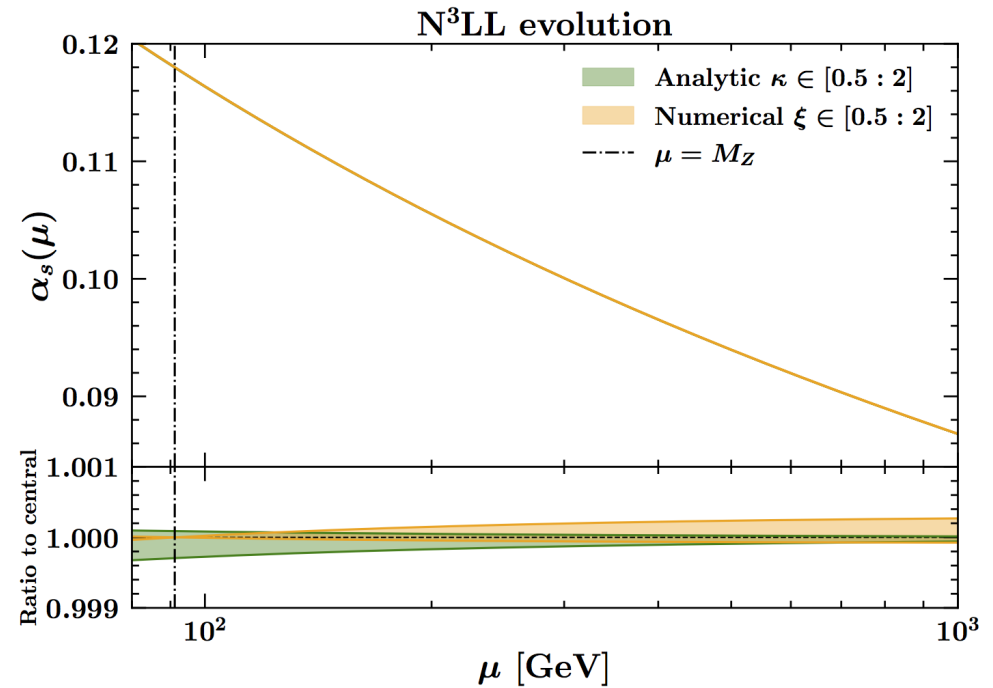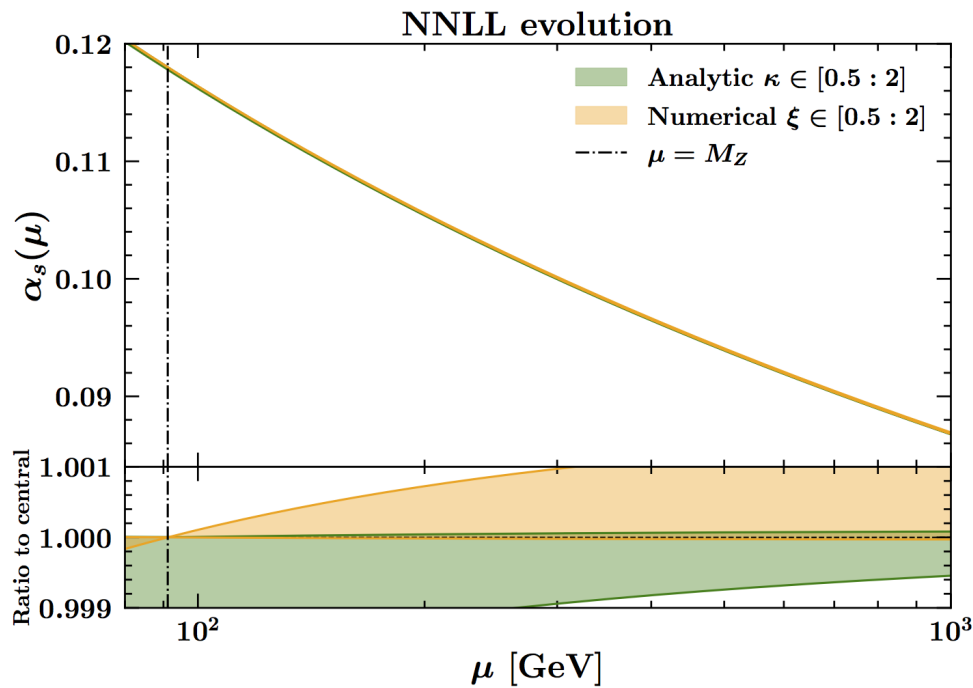
- small (per mille) effect at 1 TeV

RGE systematics of up-quark density function

F Hautmann: FCC Workshop, CERN, January 2025

- non-negligible effect – more pronounced for decreasing x (increasing energy)

RGE systematics of Sudakov form factor

- kappa and xi bands tend to align from NNLL onwards
- largest at small mu_b (i.e., at large transverse distances)

Figure 4. Analytic and numerical Sudakov form factors as functions of μ_b in the range $\mu_b \in [2 : 1000]$ GeV at NLL (top-left plot), NNLL (top-right plot), and N^{3}LL (bottom plot) accuracies. The boundary condition of the strong coupling is set at $\alpha_s(M_Z) = 0.118$. Uncertainty bands correspond to variations of the parameters κ and ξ for analytic and numerical solutions, respectively, in the range $\in [0.5 : 2]$. Lower panels display the bands normalised to the respective central-value curves obtained with $\kappa = \xi = 1$.

Impact on physical observables: F2 structure function
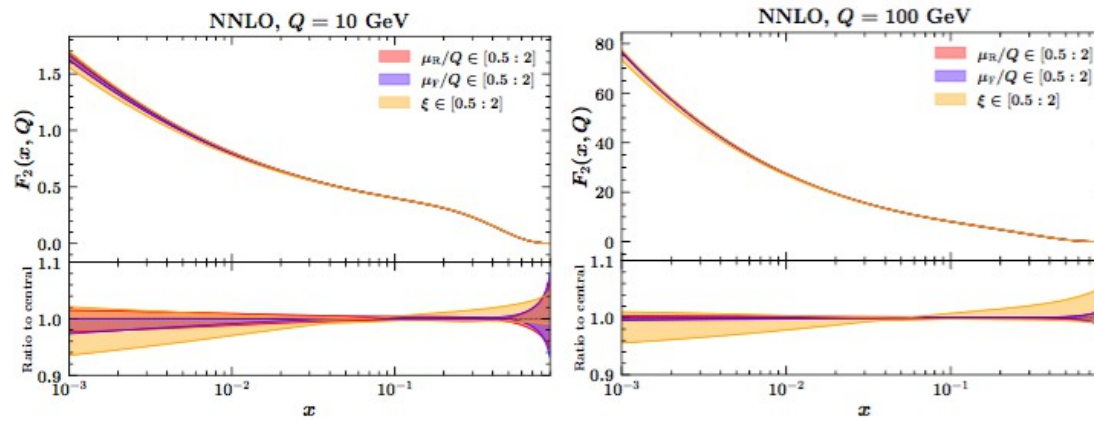
Figure 5. The DIS F_2 structure function at NNLO plotted versus x for two different values of Q. Uncertainty bands associated with variations of renormalisation and factorisation scales, μ_R and μ_F, and resummation-scale parameter, ξ, are also displayed. The lower insets show the predictions normalised to the central-scale curves.
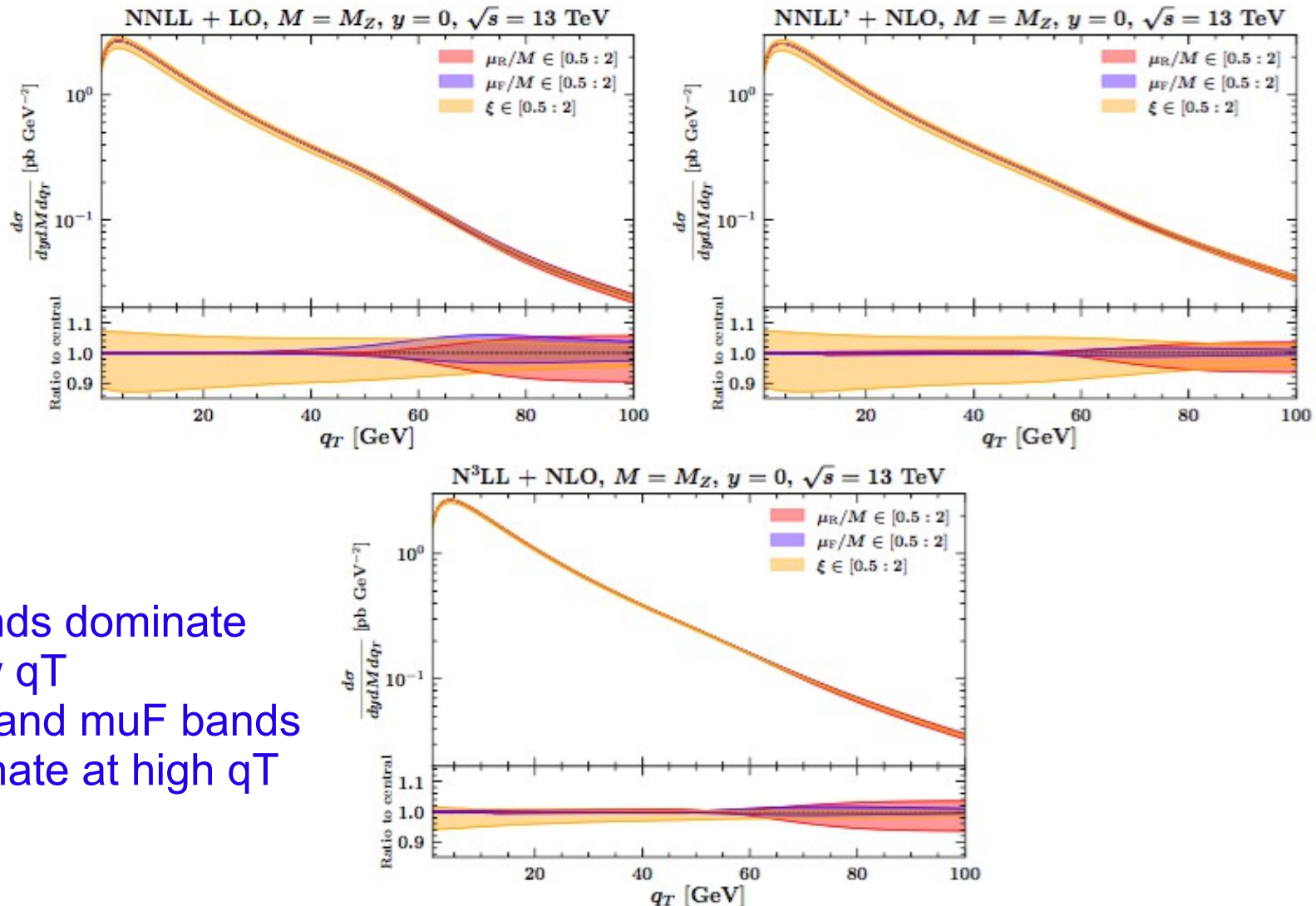
- xi band dominates at high Q
- mu bands dominate at low Q
- kinematic regions relevant for PDF extraction
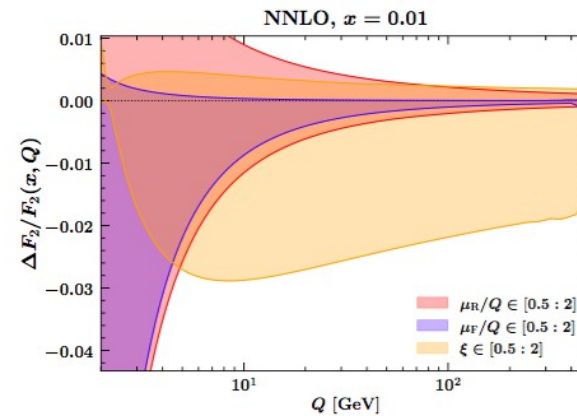
Figure 8. Q-dependence of the ratio $\Delta F_2/F_2$ at NNLO at $x = 10^{-2}$ associated with variations of renormalisation and factorisation scales, μ_R and μ_F, and resummation-scale parameter, ξ.
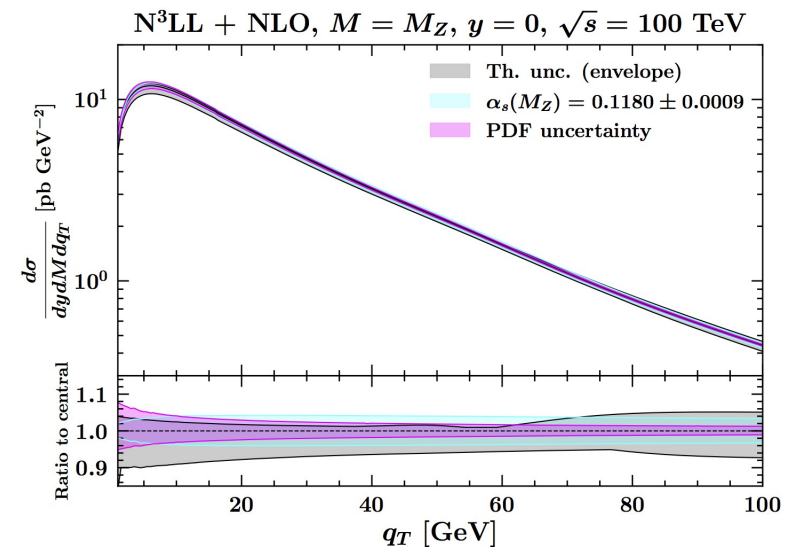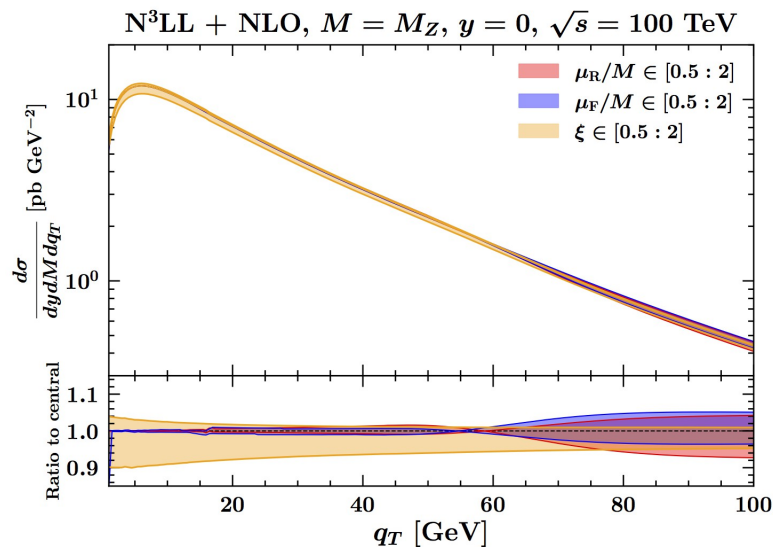
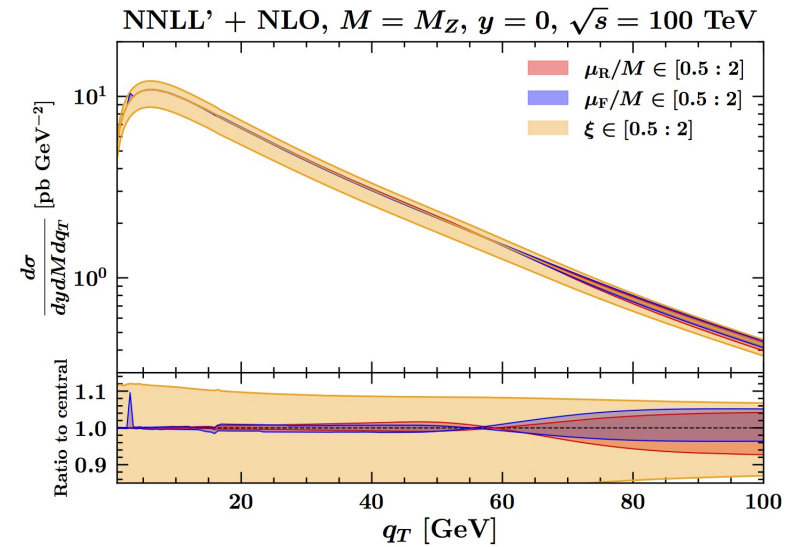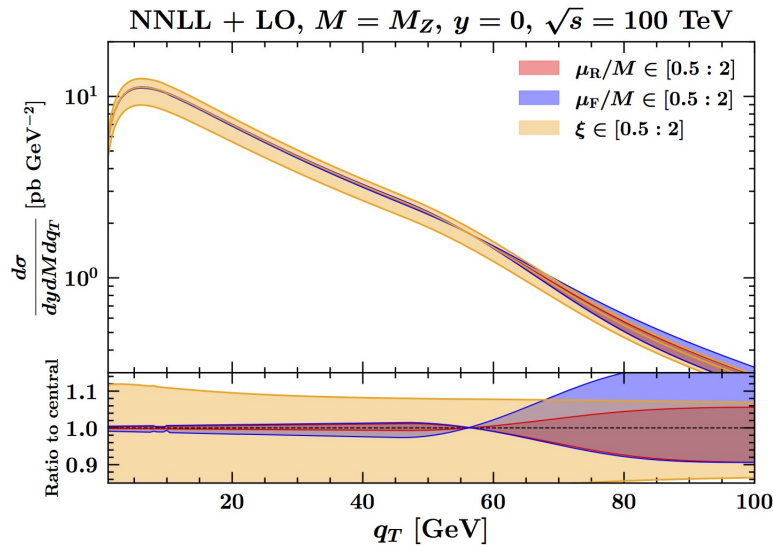# Impact on physical observables:
Z-boson transverse momentum at the LHC

- xi bands dominate at low qT
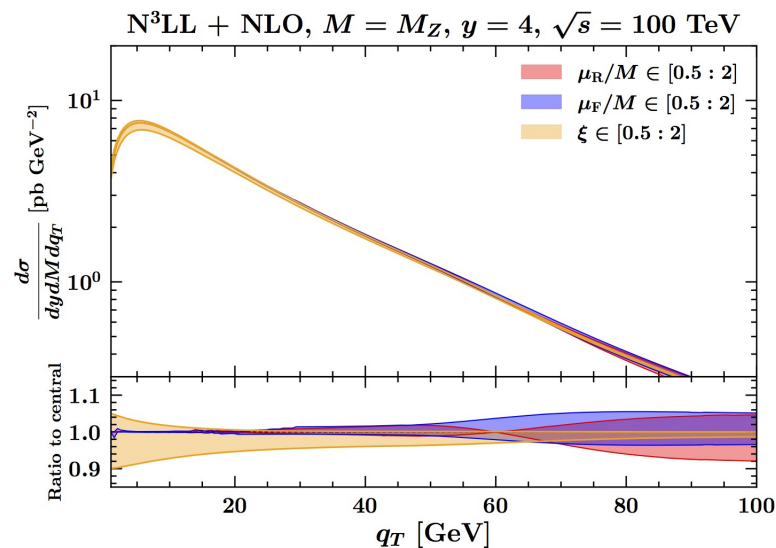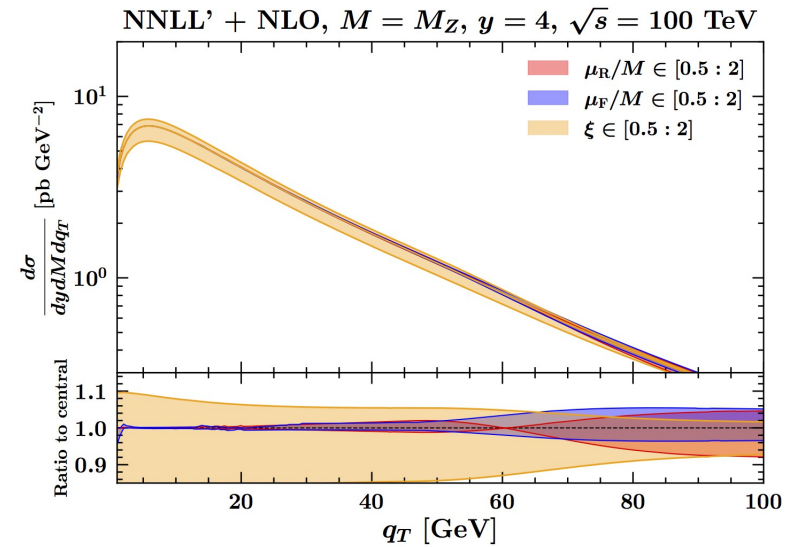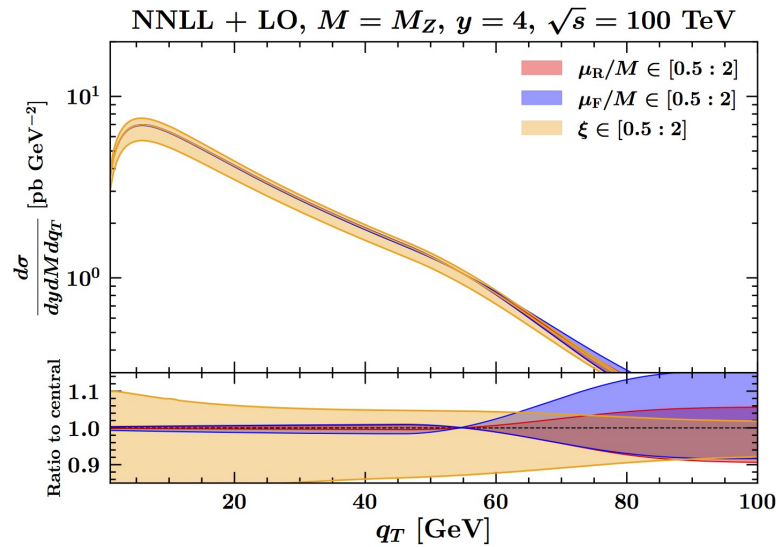- muR and muF bands dominate at high qT

Z-boson transverse momentum at the FCC-hh

RGE systematics growing with energy scale

Z-boson transverse momentum at the FCC-hh for large rapidity

NNLL + LO, $M = M_Z$, $y = 4$, $\sqrt{s} = 100$ TeV

$\frac{d\sigma}{dy\,dM\,dq_T}$ [pb GeV^{-2}]

$\mu_R/M \in [0.5:2]$
$\mu_F/M \in [0.5:2]$
$\xi \in [0.5:2]$

Ratio to central

q_T [GeV]

NNLL' + NLO, $M = M_Z$, $y = 4$, $\sqrt{s} = 100$ TeV

$\frac{d\sigma}{dy\,dM\,dq_T}$ [pb GeV^{-2}]

$\mu_R/M \in [0.5:2]$
$\mu_F/M \in [0.5:2]$
$\xi \in [0.5:2]$

Ratio to central

q_T [GeV]

N^{3}LL + NLO, $M = M_Z$, $y = 4$, $\sqrt{s} = 100$ TeV

$\frac{d\sigma}{dy\,dM\,dq_T}$ [pb GeV^{-2}]

$\mu_R/M \in [0.5:2]$
$\mu_F/M \in [0.5:2]$
$\xi \in [0.5:2]$

Ratio to central

q_T [GeV]

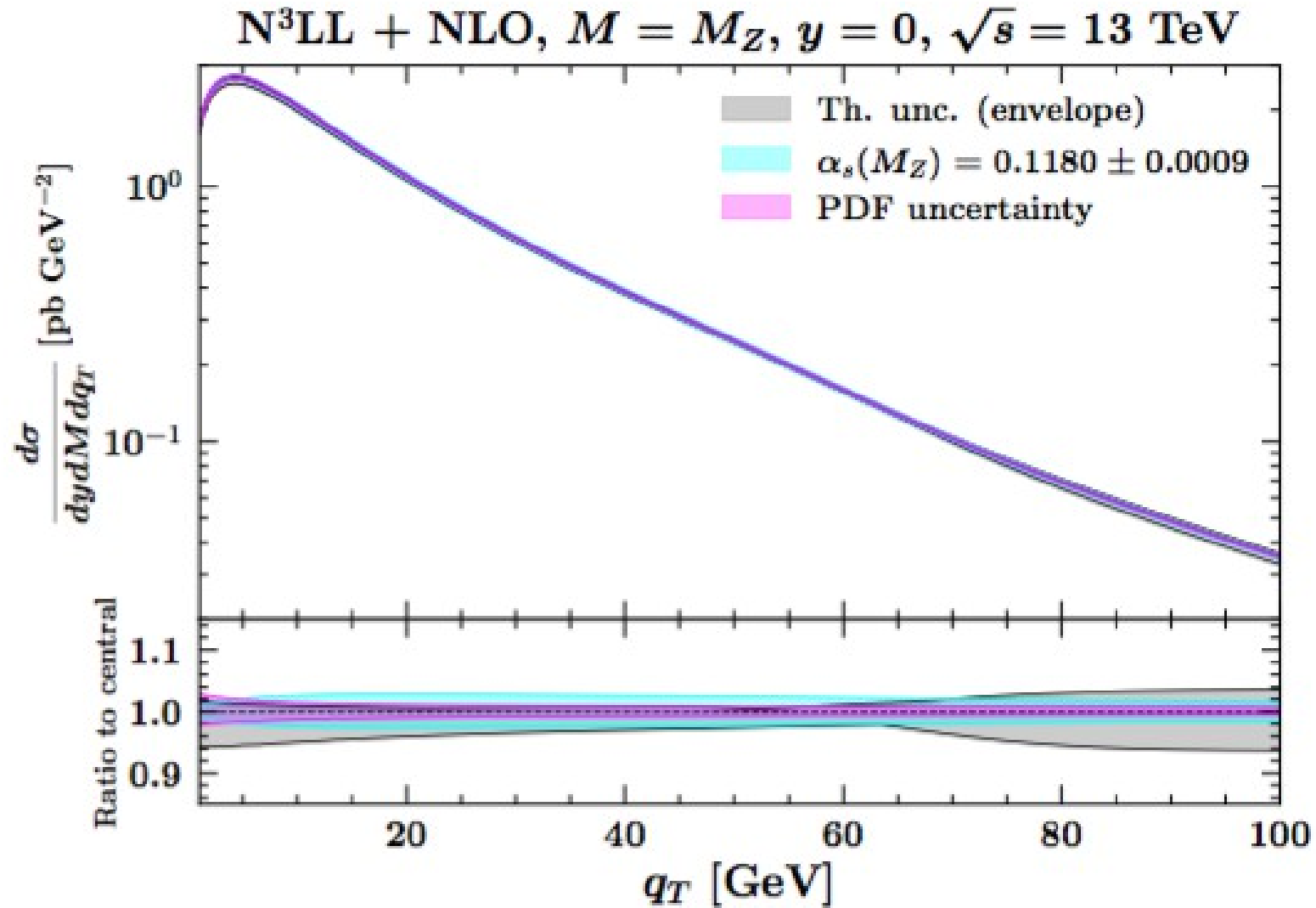- Significant production rates at large rapidities

- RGE theory uncertainties dominant at low qT
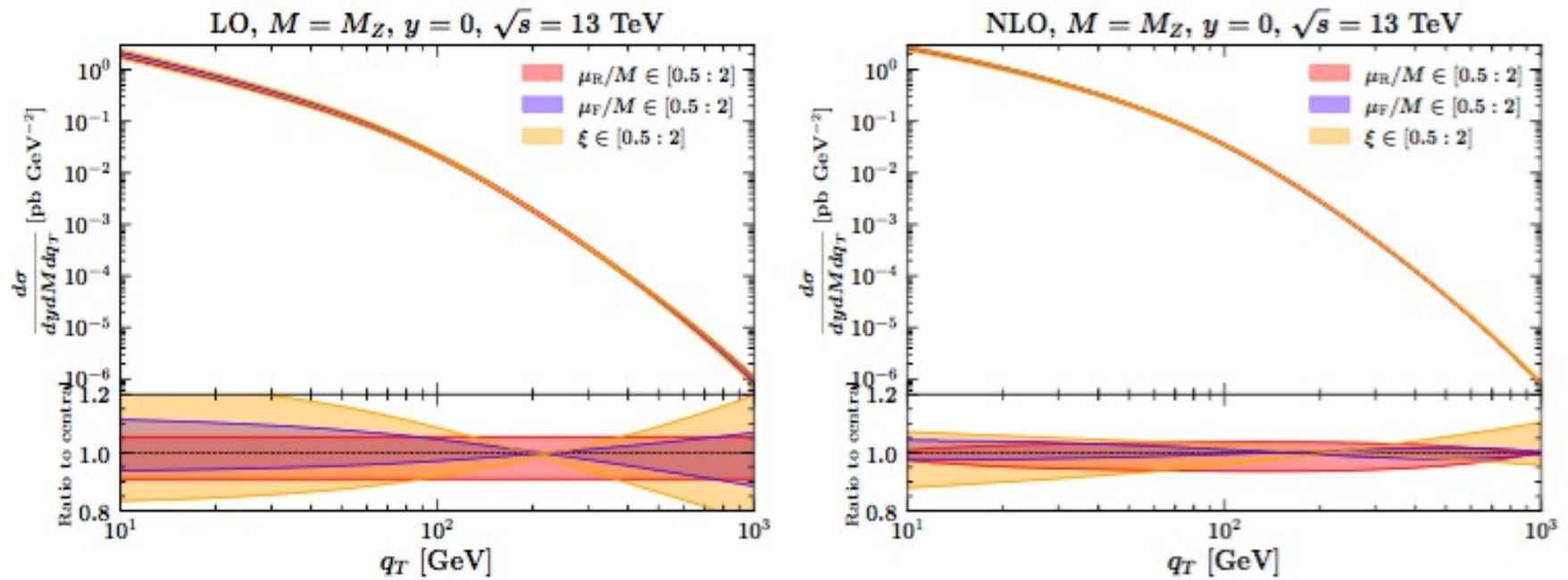
Concluding remarks

- The difference between exact and perturbative solutions to RGE, in many common single-logarithmic problems (such as the evolution of QCD coupling and PDFs) as well as in double-logarithmic problems (such as Sudakov processes), can be accounted for by variations of resummation scales.

- Such variations should be performed to assess theory uncertainties associated with RGE subleading-order terms.

- In many applications relevant for collider physics, notably the extraction of PDFs from global fits, these variations are commonly not performed. Theory uncertainties are thus not included, or underestimated. This points to the need for PDF extractions which include RGE theory uncertainties, e.g. by the use of the resummation scale technique described here.

- RGE systematic effects become more pronounced with growing mass scale and decreasing x. They are already significant at the LHC in particular phase space regions, and their importance will grow at the FCC-hh.

- The methodology presented could be applied to fragmentation and final-state QCD evolution, relevant also for FCC-ee.

Back-up slides

Z-boson transverse momentum at the LHC: theory uncertainty envelope


$N^3LL + NLO, M = M_Z, y = 0, \sqrt{s} = 13$ TeV

Legend:
- Th. unc. (envelope)
- $\alpha_s(M_Z) = 0.1180 \pm 0.0009$
- PDF uncertainty

y-axis: $\frac{d\sigma}{dy\,dM\,dq_T}$ [pb GeV^{-2}]

Ratio to central

x-axis: q_T [GeV]

Z-boson transverse momentum at large qT

Figure 9. DY large-q_T spectrum of a lepton pair with invariant mass M equal to M_Z and central rapidity ($y = 0$) at LO (left) and NLO (right) accuracies at the 13 TeV LHC. The curves include uncertainty bands associated with variations of resummation scale-parameter ξ, renormalisation scale μ_R, and factorisation scale μ_F. The upper insets display the cross sections, while the lower insets show their ratios to central-scale predictions.

RGE systematics of valence quark density
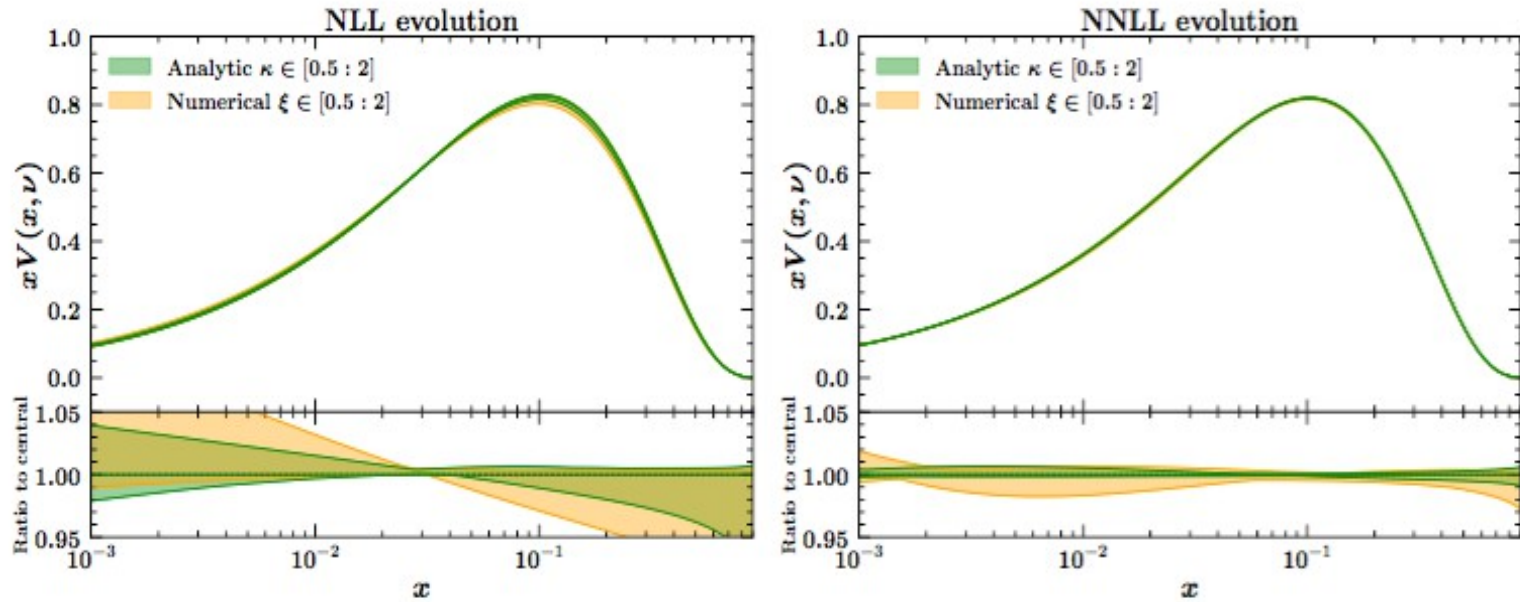
Figure 2. Total-valence PDF xV at $\nu = 100$ GeV evolved analytically and numerically, at NLL (left plot) and NNLL (right plot) accuracy, displayed over the range $x \in [10^{-3} : 1]$. The boundary-condition distributions at $\nu_0 = \sqrt{2}$ GeV and all other theory settings are taken from Ref. [74]. Uncertainty bands correspond to variations of the parameters κ and ξ for analytic and numerical solutions, respectively, in the ranges $\kappa, \xi \in [0.5 : 2]$. Lower panels display the bands normalised to the respective central-value curves obtained with $\kappa = \xi = 1$.

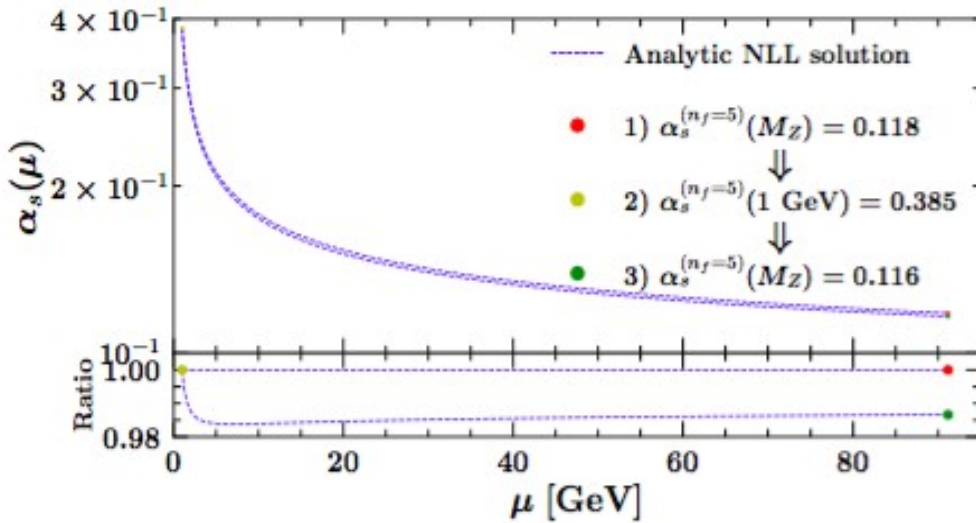# QCD coupling: hysteresis and emergent resummation scales

FIG. 1. Perturbative hysteresis for the NLL evolution of the strong coupling α_s.
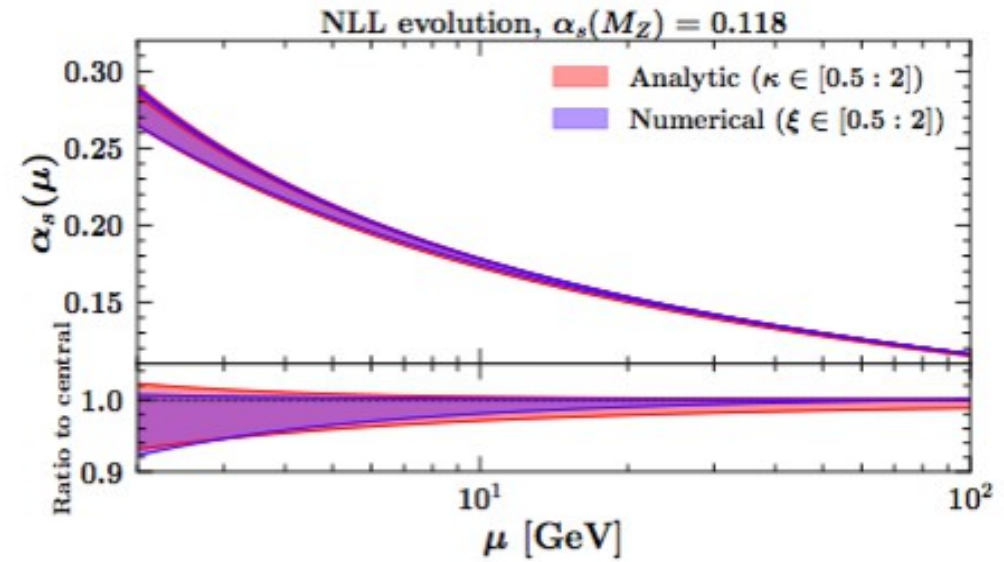

FIG. 2. Analytic and numerical evolution of the strong coupling α_s at NLL. The bands indicate the uncertainty computed by varying the factors κ and ξ in the range $[0.5:2]$.

- *Loop from mu_0 = M_Z to mu = 1 GeV back to mu_0 = M_Z: alpha_s, given by the NLL solution in Eq.(5), does not return to the original value.*
This is the known hysteresis effect in RGE perturbative solutions.

- *Hysteresis is here traced back to RGE theory uncertainties due to uncalculated subleading orders in the evolution kernels.*
This can be evaluated by using the "emergent resummation scale" technique.

22

Implications for the structure function F2

- *Relative variation Delta-F2 / F2 as a function of Q, from resummation scales and renormalization/factorization scales*
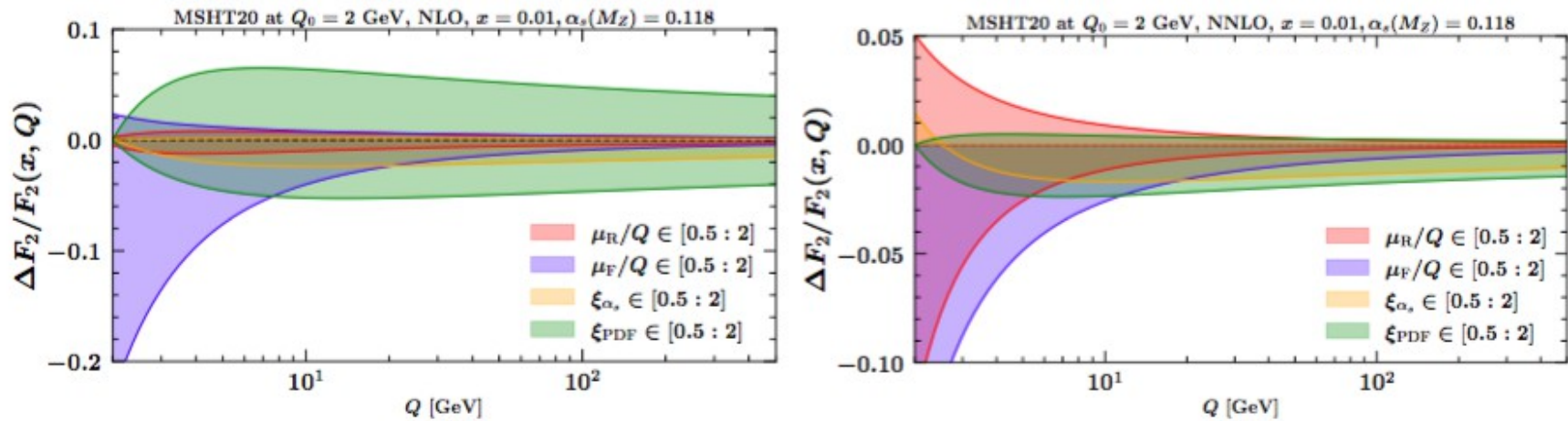

FIG. 6. Q-dependence of the relative variation $\Delta F_2/F_2$ at NLO and NNLO associated with variations of renormalisation and factorisation scales, μ_R and μ_F, and resummation scales ξ_{α_s} and ξ_{PDF}.

- The xi_PDF contribution starts from 0 and grows rapidly with Q, remaining sizeable out to large Q, while the mu_F contribution is largest at low Q and decreases with increasing Q.

- Analogously, the mu_R contribution is important at low Q and decreases with Q, while the xi_alpha is subdominant at low Q but becomes relevant at high Q.

- The xi_PDF contribution stays comparatively significant for large Q and small x, corresponding to higher-order perturbative corrections to PDF anomalous dimensions dominating the small-x region for sufficiently large Q.